Angular correlations in internal pair conversion of aligned heavy nuclei

C. R. Hofmann* and G. Soff
Institut für Theoretische Physik, TU Dresden, D-01062 Dresden, Germany

J. Reinhardt† and W. Greiner
Institut für Theoretische Physik, J. W. Goethe Universität, D-60054 Frankfurt am Main, Germany
(Received 5 September 1995)

We calculate the spatial correlation of electrons and positrons emitted by internal pair conversion of Coulomb excited nuclei in heavy-ion collisions. The alignment of the nucleus results in an anisotropic emission of the electron-positron pairs that is closely related to the anisotropic emission of γ rays. However, the angular correlation in the case of internal pair conversion displays additional features which provide the possibility for a deeper understanding of the nuclear structure. Our results are of particular interest for the electron-positron coincidence experiments currently analyzed at GSI (Darmstadt) and at Argonne. [S0556-2813(96)03505-4]

PACS number(s): 23.20.Nx, 25.70.De

I. INTRODUCTION

Heavy-ion collisions at energies in the vicinity of the nuclear Coulomb barrier lead to an alignment of the colliding nuclei. This implies that the magnetic substates are no longer equally populated. To describe deexcitation processes following heavy-ion collisions such as γ-ray emission or internal conversion, we have to account for this specific population by weighting the transition matrix elements with the occupation probability of, rather than just averaging over, the decaying substates.

The population of the various nuclear substates is incorporated in the formalism by introducing the density matrix of the excited quantum system or, in the case of rotational symmetry of the problem, by a set of statistical tensors which obey the same transformation law as the spherical harmonics. This concept enables us to treat the polarization or alignment of excited nuclei appropriately. First calculations of the angular correlation of electrons and positrons emitted in internal pair conversion taking into account the alignment of nuclei were accomplished by Goldring [1], Rose [2], and Warburton [3]. These calculations were performed within Born approximation, neglecting the influence of the nuclear charge on the outgoing electron and positron. But for internal pair conversion (IPC) of highly charged nuclei, the Born approximation is not justified as can be verified by the corresponding positron spectra [4–6].

Therefore we reconsider in the following the internal pair conversion of heavy nuclei which are aligned, e.g., by Coulomb excitation or transfer reactions. We determine the angular correlation of the emitted electron and positron with respect to a reference axis in space. As already known for the angular correlation of γ rays, the problem will be simplified if we choose a coordinate system in which the density matrix is diagonal. The statistical tensors depend as well on the choice of the coordinate system. If the entries of the statistical tensors are given in a specific coordinate system, we are able to calculate the angular correlation with respect to the z axis of this system.

The occupation probabilities of the magnetic substates caused by Coulomb excitation can be calculated with, e.g., the COULEX code of Alder and Winther [7]. However, one should take into account the change of population by electromagnetic transitions from higher-lying states. Special attention should be paid to a proper choice of the coordinate system when dealing with the COULEX code [7,8]. For pure Coulomb excitation we will assume the z axis to point along the asymptotic target recoil axis. With respect to this axis the excited nuclei may exhibit prolate or oblate alignment.

Our investigations are particularly relevant for the understanding and interpretation of the electron-positron coincidence experiments which are presently performed by the EPOS and ORANGE groups at the UNILAC collider of GSI (Darmstadt) [9] and by the APEX collaboration at Argonne [10]. These experimental setups were designed to measure the production rate of electron-positron pairs emitted in heavy-ion collisions with ion energies close to the nuclear Coulomb barrier. The experimental devices allow one to detect electrons and positrons as well as γ rays in coincidence with the scattered ions, enabling also the determination of the corresponding relative angles. For the analysis and understanding of the experimental spectra, one relies on information of all the processes which can cause the formation of electron-positron pairs. Here the internal pair conversion contributes typically between 20% up to 80% of the total pair production yield.

II. DENSITY MATRIX AND STATISTICAL TENSORS

The density matrix—and for spherical symmetry the set of statistical tensors—is the appropriate tool for including statistical properties such as occupation probabilities of quantum mechanical states into the calculations. Here we briefly summarize the essential properties of the density matrix and subsequently turn to the concept of the statistical tensors, which obey the same transformation law as irreducible tensors. For the density matrix $\rho_{M_i M_i'}(J_i)$ of dimension $(2J_i+1)\times(2J_i+1)$, we note the following.

*Electronic address: hofmann@ptprs8.phy.tu-dresden.de
†Electronic address: jr@th.physik.uni-frankfurt.de

(1) The density matrix is Hermitian:

$$\rho^{*}_{M_i' M_i}(J_i) = \rho_{M_i M_i'}(J_i).$$

(2) The trace of the density matrix equals 1:

$$\mathrm{Tr}\{\rho\} = 1 \Leftrightarrow \sum_{M_i} \rho_{M_i M_i}(J_i) = 1.$$

(3) $\mathrm{Tr}\{\rho^2\} \leqslant 1$ and $\mathrm{Tr}\{\rho^2\} = 1 \Leftrightarrow$ the system is in a pure state.

We define the statistical tensors $\hat{\rho}^{[n]}_{\nu}$ as irreducible tensors of rank n with $\nu = -n, \ldots, n$:

$$\hat{\rho}^{[n]}_{\nu}(J_i) = \sum_{M_i, M_i'} (-1)^{J_i - M_i'} \sqrt{2n+1} \begin{pmatrix} J_i & J_i & n \\ M_i & M_i' & -\nu \end{pmatrix} \times \rho_{M_i M_i'}(J_i). \tag{1}$$

The argument J_i reminds us that n is related to the angular momentum of the magnetic substates by $0 \leqslant n \leqslant 2J_i$. From the normalization of the density matrix, it follows that $\hat{\rho}^{[0]}_0(J_i) = 1/\sqrt{2J_i+1}$.

The density matrix has $(2J_i+1)^2$ independent components. To describe a system by statistical tensors instead of the density matrix, we need $2J_i+1$ density tensors of rank $n=0$ up to rank $n=2J_i$. Since the density tensor of rank n has $2n+1$ components, we get again $\Sigma^{2J_i}_{n=0}(\Sigma^{n}_{\nu=-n}1) = (2J_i+1)^2$ independent components.

The statistical tensors transform under rotations according to

$$\hat{\rho}^{[n]}_{\nu}(J_i) = \sum_{\nu'} \mathscr{D}^{[n]*}_{\nu'\nu}(\vec{\alpha}) \hat{\rho}^{[n]}_{\nu'}(J_i), \tag{2}$$

where the Wigner rotation matrix of rank n is denoted by $\mathscr{D}^{[n]}$ and the set of Euler angles by $\vec{\alpha}$. In defining the Euler angles we follow Rose [11] and Eisenberg and Greiner [12]. For systems with rotational symmetry it is thus more advantageous to employ the concept of the statistical tensors when incorporating statistical statements concerning the system. The components of the statistical tensors are changed under rotations and so are the occupation numbers of the magnetic substates.

From the set of $2J_i+1$ statistical tensors, we obtain the density matrix by utilizing the relation

$$\rho_{M_i M_i'}(J_i) = (-1)^{J_i - M_i'} \sum_{n,\nu} \sqrt{2n+1} \times \begin{pmatrix} J_i & J_i & n \\ M_i' & -M_i & -\nu \end{pmatrix} \hat{\rho}^{[n]}_{\nu}(J_i). \tag{3}$$

For certain symmetries of the system we can reduce the independent components of the statistical tensors. Here we list the consequences for the statistical tensors in three special cases which will become relevant for us.

(1) In the case of *axial symmetry* the density matrix is diagonal and its diagonal components are just the probabilities for the occupation of the corresponding magnetic substates $\rho_{M_i M_i} = p_{M_i}$:

$$\hat{\rho}^{[n]}_{\nu}(J_i) = \delta_{0\nu} \sum_{M_i} (-1)^{J_i - M_i} p_{M_i} \begin{pmatrix} J_i & J_i & n \\ M_i & -M_i & 0 \end{pmatrix}.$$

One can always choose a basis such that the density matrix is diagonal, but in general this will not be a basis of wave functions with good angular momentum.

(2) In the case of *spherical symmetry*, there is no direction singled out in space. The density matrix is proportional to the identity matrix. The diagonal elements are given by $\rho_{M_i M_i} = 1/(2J_i+1)$. All statistical tensors vanish with exception of the tensor of rank 0, i.e.,

$$\hat{\rho}^{[n]}_{\nu}(J_i) = \delta_{0n}\delta_{0\nu} \frac{1}{\sqrt{2J_i+1}}.$$

(3) From Eq. (1) it can be shown that for alignment of the nuclear states, defined by $p_{M_i} = p_{-M_i}$, the statistical tensors of odd rank vanish.

III. ANGULAR CORRELATION OF γ RAYS

Before we enter into the calculations concerning the angular correlation in internal pair conversion, we summarize some results already known for in-beam γ-ray spectroscopy. This will help us to interpret the angular correlation pattern in the case of internal pair conversion. The angular correlation of photons emitted after Coulomb excitation is essentially determined by the statistical tensors, i.e., by the occupation numbers of the magnetic substates of the decaying nucleus. In choosing a reference axis for which the density matrix is diagonal, just the zeroth components of all statistical tensors survive and we obtain for the transition probability the well-known relations

$$\frac{dP_\gamma}{d\Omega} = \frac{2\alpha\omega}{\sqrt{2J_i+1}} |V^{(\tau)}_\gamma(L)|^2 \sum_{I\ \mathrm{even}} F_I(LLJ_fJ_i) \times \hat{\rho}^{[I]}_0(J_i) P_I(\cos\vartheta) \tag{4}$$

for a transition of parity $\tau = E/M$ and multipolarity L. $V^{(\tau)}_\gamma(L)$ denotes the corresponding reduced matrix element for the nuclear transition. Here we employed the correlation coefficients [13–15]

$$F_I(LLJ_fJ_i) = (-)^{J_f + J_i - 1} \sqrt{2I+1}\sqrt{2J_i+1}(2L+1) \times \begin{pmatrix} L & L & I \\ 1 & -1 & 0 \end{pmatrix} \begin{Bmatrix} L & L & I \\ J_i & J_i & J_f \end{Bmatrix}. \tag{5}$$

This results in an anisotropic emission of photons with respect to the alignment axis. The number of minima of the angular distribution corresponds to the multipolarity of the nuclear transition.

In the case of spherical symmetry, the photon emission is isotropic,

$$\frac{dP_\gamma}{d\Omega} = \frac{2\alpha\omega}{2J_i+1} |V^{(\tau)}_\gamma(L)|^2, \tag{6}$$

or integrated over the solid angle Ω,

$$P_\gamma = \frac{8\pi\alpha\omega}{2J_i+1}\,|V_\gamma^{(\tau)}(L)|^2. \tag{7}$$

IV. TRANSITION PROBABILITIES FOR INTERNAL PAIR CONVERSION

We turn now to the formulation of the triple correlation of the electron and positron directions with reference to a symmetry axis, which is taken as quantization axis.

For a statistical ensemble of nuclei, we write the transition probability for internal pair conversion,

$$P_{e^+e^-} = 2\pi \sum_{M_i,M_i',M_f,\lambda,\lambda'} \int d^3p \int d^3p' \times \delta(\omega - W' - W)\, U_{\rm pl}\rho_{M_iM_i'}U_{\rm pl}^*, \tag{8}$$

where the density matrix $\rho_{M_iM_i'}$ represents the occupation of the magnetic substates $|J_iM_i\rangle$. Here we assumed a nuclear transition from an initial state $|J_iM_i\rangle$ to the final state $|J_fM_f\rangle$ where the initial state is populated according to the density matrix $\rho_{M_iM_i'}$. Since we do not require the density matrix to be diagonal, the summation extends over both M_i and M_i'. The δ function ensures energy conservation: The transition energy ω is transferred to the electron (total energy W') and to the positron (total energy W). The summation is taken over the spins and the momenta of the outgoing leptons.

The matrix element for internal pair conversion is written in lowest order of α in the retarded form

$$U_{\rm pl} = -\alpha \int dV_n \int dV_e [\rho_n(\vec r_n)\rho_e(\vec r_e) - \vec j_n(\vec r_n)\cdot\vec j_e(\vec r_e)] \times \frac{e^{i\omega|\vec r_n - \vec r_e|}}{|\vec r_n - \vec r_e|}, \tag{9}$$

$\vec r_e$ being the electronic coordinate and $\vec r_n$ the nuclear coordinate.

Since we neglect in our work the penetration of the electron wave functions, we do not have to specify the nuclear transition charge and current densities ρ_n and j_n. The electronic transition charge and current densities read

$$\rho_e = \psi_f^\dagger\psi_i, \quad \vec j_e = \psi_f^\dagger\vec\alpha\psi_i \tag{10}$$

($\vec\alpha$ is the three vector of the spatial Dirac matrices in the standard representation). These expressions are evaluated utilizing the scattering solutions [see Eqs. (A5) and (A8) in Appendix A] for the electron and positron wave functions in order to define the emission direction and thus an opening angle. Inserting the spherical wave expansion of these wave functions results in a decomposition of the matrix element, Eq. (9),

$$U_{\rm pl} = \sum_{\kappa',\mu'} \sum_{\kappa,\mu} a_{\kappa'\mu'}^{(-)*} b_{\kappa\mu}^{(+)} U_{\kappa'\mu'\kappa\mu}. \tag{11}$$

$U_{\kappa'\mu'\kappa\mu}$ denotes the transition matrix element which has the same structure as $U_{\rm pl}$, but is evaluated using the spherical spinor solutions of the Dirac equation, Eq. (A1). This matrix element was calculated in [5]. Here we cite the result:

$$U_{\kappa'\mu'\kappa\mu} = 4\pi i\alpha\omega(-1)^{J_f-M_f}\begin{pmatrix} J_f & L & J_i \\ -M_f & M & M_i\end{pmatrix} V_\gamma^{(\tau)}(L) \times (-1)^{j'-\mu'}\begin{pmatrix} j' & L & j \\ -\mu' & M & \mu\end{pmatrix} M_{\kappa'\kappa}^{(\tau)}(L). \tag{12}$$

$V_\gamma^{(\tau)}(L)$ is just the reduced nuclear matrix element of Eq. (7), and

$$M_{\kappa'\kappa}^{(\tau)}(L) = -i(-1)^{j'+1/2}\frac{\sqrt{2j+1}\sqrt{2j'+1}\sqrt{2L+1}}{4\pi\sqrt{L(L+1)}} \times \begin{pmatrix} j & j' & L \\ -1/2 & 1/2 & 0\end{pmatrix} R_{\kappa'\kappa}^{(\tau)}, \tag{13}$$

with the parity selection rule

$$l + l' + L + \lambda(\tau) = 0 \mod 2 \begin{cases} \lambda = 0 & \text{for } \tau = \text{electric}, \\ \lambda = 1 & \text{for } \tau = \text{magnetic}. \end{cases} \tag{14}$$

$R_{\kappa'\kappa}^{(\tau)}$ contains the integration over the radial electron wave functions and will be defined later.

Inserting this matrix element into the pair conversion probability, Eq. (8), yields

$$P_{e^+e^-} = 2\pi \sum_{M_i,M_i',M_f} \rho_{M_iM_i'}^{[J_i]} \sum_{\lambda,\lambda'} \int dW\, d\Omega \times \int dW'\, d\Omega'\, \delta(\omega - W' - W) \sum_{\kappa',\mu'} \sum_{\kappa,\mu} \sum_{\overline{\kappa'},\overline{\mu'}} \times \sum_{\overline{\kappa\mu}} A_{\kappa',\mu';\overline{\kappa'}\,\overline{\mu'}} B_{\kappa\mu;\overline{\kappa\mu}} U_{\kappa'\mu'\kappa\mu} U^*_{\overline{\kappa'}\,\overline{\mu'}\,\overline{\kappa\mu}}, \tag{15}$$

where we abbreviated

$$A_{\kappa'\mu';\overline{\kappa'}\,\overline{\mu'}} = W'p' \sum_{\lambda'} a_{\kappa'\mu'}^{(-)*} a_{\overline{\kappa'}\,\overline{\mu'}}^{(-)} \tag{16}$$

and

$$B_{\kappa\mu;\overline{\kappa\mu}} = Wp \sum_{\lambda} b_{\kappa\mu}^{(+)} b_{\overline{\kappa\mu}}^{(+)*}. \tag{17}$$

From Eq. (15) we obtain the differential pair conversion probability with respect to the *kinetic positron energy* $E = W - m$ and the solid angles of both electron, Ω', and positron, Ω,

$$P_{e^+e^-} = \int_0^{\omega-2m} dE \int d\Omega \int d\Omega'\, \frac{d^3P_{e^+e^-}}{dE\, d\Omega\, d\Omega'}. \tag{18}$$

The integration over the electron energy W' is trivially performed because of the δ function. From this relation it is obvious that we may proceed from the solid angles Ω to $\widetilde\Omega$

by choosing another reference axis in space. The integrand in Eq. (18) is invariant under rotations since the Jacobian of this transformation equals 1. The integrand should thus be represented by a series of triple correlation functions, which are defined in Eq. (22).

Inserting the explicit expressions of the coefficients A and B, Eqs. (B2) and (B4), leads to the following expression for the differential pair conversion probability:

$$\frac{d^3P_{e^+e^-}}{dE\ d\Omega\ d\Omega'} = 8(\pi\alpha\omega)^2 |V_\gamma^{(\tau)}(L)|^2 \sum_{M,M} \sum_{M_i,M_i'} \sum_{M_f} \rho^{[J_i]}_{M_iM_i'} \begin{pmatrix} J_f & L & J_i \\ -M_f & M & M_i \end{pmatrix} \begin{pmatrix} J_f & L & J_i \\ -M_f & M & M_i' \end{pmatrix} \sum_{\kappa,\kappa',\overline{\kappa\kappa'}} (-1)^{j'+\overline{j'}}$$
$$\times M^{(\tau)}_{\kappa'\kappa}(L) M^{(\tau)*}_{\overline{\kappa'}\overline{\kappa}}(L) \sqrt{2\overline{j'}+1}\sqrt{2j'+1}\sqrt{2j+1}\sqrt{2\overline{j}+1} \exp\{i[\delta'(W',\kappa') - \overline{\delta'}(W',\overline{\kappa'}) + \delta(-W,\kappa)$$
$$- \overline{\delta(-W,\overline{\kappa})}]\} \sum_{I',I,\alpha,\alpha'} \sqrt{2I'+1}\sqrt{2I+1} Y_{I'\alpha'}(\Omega_{p'}) Y_{I\alpha}(\Omega_p) \begin{pmatrix} j' & \overline{j'} & I' \\ 1/2 & -1/2 & 0 \end{pmatrix} \begin{pmatrix} j & \overline{j} & I \\ 1/2 & -1/2 & 0 \end{pmatrix}$$
$$\times \sum_{\mu,\mu',\overline{\mu},\overline{\mu'}} (-1)^{\overline{\mu}-\overline{\mu'}+1} \begin{pmatrix} \overline{j'} & L & \overline{j} \\ -\overline{\mu'} & M & \overline{\mu} \end{pmatrix} \begin{pmatrix} j' & L & j \\ -\mu' & M & \mu \end{pmatrix} \begin{pmatrix} \overline{j'} & j' & I' \\ -\overline{\mu'} & \mu' & -\alpha' \end{pmatrix} \begin{pmatrix} \overline{j} & j & I \\ -\overline{\mu} & \mu & \alpha \end{pmatrix}. \tag{19}$$

Here we inserted Eq. (12). Introducing the statistical tensors we are left with

$$\frac{d^3P_{e^+e^-}}{dE\ d\Omega\ d\Omega'} = 2(4\pi\alpha\omega)^2 |V_\gamma^{(\tau)}(L)|^2 (-1)^{J_f-J_i+L+1} \sum_{n,\nu} \sqrt{2n+1}(-1)^\nu \hat{\rho}^{[n]}_\nu(J_i) \begin{Bmatrix} L & L & n \\ J_i & J_i & J_f \end{Bmatrix} \sum_{I,I'} \sqrt{2I+1}\sqrt{2I'+1}$$
$$\times (-1)^{I'} \sum_{\alpha,\alpha'} Y_{I'\alpha'}(\Omega_{p'}) Y_{I\alpha}(\Omega_p) \begin{pmatrix} I & I' & n \\ \alpha & \alpha' & -\nu \end{pmatrix} \sum_{\kappa,\kappa',\overline{\kappa},\overline{\kappa'}} (-1)^{\overline{j}+\overline{j'}} \sqrt{|\kappa\kappa'\overline{\kappa}\overline{\kappa'}|} \begin{Bmatrix} \overline{j} & \overline{j'} & L \\ j & j' & L \\ I & I' & n \end{Bmatrix} M^{(\tau)}_{\kappa'\kappa}(L)$$
$$\times M^{(\tau)*}_{\overline{\kappa'}\overline{\kappa}}(L) \exp\{i[\delta'(E',\kappa') - \overline{\delta'}(E',\overline{\kappa'}) + \delta(-E,\kappa) - \overline{\delta(-E,\overline{\kappa})}]\} \begin{pmatrix} j' & \overline{j'} & I' \\ 1/2 & -1/2 & 0 \end{pmatrix} \begin{pmatrix} j & \overline{j} & I \\ 1/2 & -1/2 & 0 \end{pmatrix}. \tag{20}$$

This is the most general form for the pair conversion probability. Now we assume that we are dealing with internal pair conversion of aligned nuclei ($\nu=0$). We may choose an appropriate coordinate system by transformation of the spherical harmonics:

$$Y_{I\alpha}(\Omega_p) = \sum_\beta \exp(i\alpha\phi) d^{[I]}_{\alpha\beta}(\vartheta) \exp(i\beta\delta) Y_{I\beta}(0,0)$$
$$= \sqrt{\frac{2I+1}{4\pi}} \exp(i\alpha\phi) d^{[I]}_{\alpha 0}(\vartheta),$$

$$Y_{I'-\alpha}(\Omega_{p'}) = \sum_{\beta'} \exp(-i\alpha\phi) d^{[I']}_{-\alpha\beta'}(\vartheta) \exp(i\beta'\delta) Y_{I'\beta'}(\Theta,0). \tag{21}$$

Here Θ denotes the opening angle of the electron-positron pair, ϑ is the polar angle of the positron with respect to the symmetry axis, and the dihedral angle δ indicates the rotation of the electron-positron plane around the positron axis [Fig. 2(b)]. Please note that the convention of [1–3] differs in the definition of the angles from the one employed here.

This enables us to define the triple correlation function by

$$P_{II'n}(\vartheta,\Theta,\delta) = \sum_\alpha \begin{pmatrix} I & I' & n \\ \alpha & -\alpha & 0 \end{pmatrix} Y_{I\alpha}(\Omega_p) Y_{I'-\alpha'}(\Omega_{p'})$$
$$= \frac{\sqrt{2I+1}\sqrt{2I'+1}}{4\pi} \sum_{\beta'} (-1)^{\beta'} \begin{pmatrix} I & I' & n \\ 0 & \beta' & \beta' \end{pmatrix} d^{[n]}_{\beta' 0}(\vartheta) d^{[I']}_{\beta' 0}(\Theta) \exp(i\beta'\delta). \tag{22}$$

Our triple correlation function is related to the one introduced by Biedenharn [13] by a factor $4\pi i^{-I-I'-n}/[(2I+1)(2I'+1)]^{1/2}$.

The pair conversion probability is normalized by the probability for γ emission, Eq. (7), which yields the pair conversion coefficient

$$\frac{d^4\beta}{dE\ d\cos\Theta d\cos\vartheta\ d\delta}=\frac{2\alpha\omega(2L+1)}{L(L+1)}(2J_i+1)(-1)^{J_f-J_i+L+1}\sum_n\sqrt{2n+1}\hat{\rho}_0^{[n]}(J_i)\begin{Bmatrix}L & L & n\\ J_i & J_i & J_f\end{Bmatrix}$$
$$\times\sum_{I,I'}(2I+1)(2I'+1)(-1)^{I'}\sum_{\beta'}(-1)^{\beta'}\begin{pmatrix}I & I' & n\\ 0 & \beta' & -\beta'\end{pmatrix}d^{[n]}_{\beta'0}(\vartheta)d^{[I']}_{\beta'0}(\Theta)\exp(i\beta'\delta)$$
$$\times\sum_{\kappa,\kappa',\overline{\kappa},\overline{\kappa'}}(-1)^{j+\overline{j'}}|\kappa\kappa'\overline{\kappa}\overline{\kappa'}|\begin{Bmatrix}\overline{j} & \overline{j'} & L\\ j & j' & L\\ I & I' & n\end{Bmatrix}R^{(\tau)}_{\kappa'\kappa}(L)R^{(\tau)*}_{\overline{\kappa'}\overline{\kappa}}(L)$$
$$\times\exp\{i[\delta'(W',\kappa')-\overline{\delta'}(W',\overline{\kappa'})+\delta(-W,\kappa)-\overline{\delta}(-W,\overline{\kappa})]\}$$
$$\times\begin{pmatrix}j' & \overline{j'} & I'\\ 1/2 & -1/2 & 0\end{pmatrix}\begin{pmatrix}j & \overline{j} & I\\ 1/2 & -1/2 & 0\end{pmatrix}\begin{pmatrix}j & j' & L\\ 1/2 & -1/2 & 0\end{pmatrix}\begin{pmatrix}\overline{j} & \overline{j'} & L\\ 1/2 & -1/2 & 0\end{pmatrix}. \tag{23}$$

Here we inserted the explicit expressions for the electronic matrix elements, Eq. (13). Integration over the azimuthal angle is trivially performed resulting in an additional factor of 2π.

The radial matrix elements read, for electric pair conversion [parity $(-)^L$],

$$R^{(e)}_{\kappa'\kappa}=L(R_1+R_2+R_3-R_4)+(\kappa-\kappa')(R_3+R_4) \tag{24}$$

and, for magnetic pair conversion [parity $(-)^{L+1}$],

$$R^{(m)}_{\kappa'\kappa}=(\kappa+\kappa')(R_5+R_6). \tag{25}$$

The radial integrals introduced in these equations are taken over products of the radial electron wave functions (A4) and the Hankel functions of first kind, $h^{(1)}_L(\omega r)$:

$$R_1=\int_0^\infty dr\ r^2 g_{W',\kappa'}(r)g_{-W,\kappa}(r)h^{(1)}_L(\omega r),$$
$$R_2=\int_0^\infty dr\ r^2 f_{W',\kappa'}(r)f_{-W,\kappa}(r)h^{(1)}_L(\omega r),$$
$$R_3=\int_0^\infty dr\ r^2 g_{W',\kappa'}(r)f_{-W,\kappa}(r)h^{(1)}_{L-1}(\omega r),$$
$$R_4=\int_0^\infty dr\ r^2 f_{W',\kappa'}(r)g_{-W,\kappa}(r)h^{(1)}_{L-1}(\omega r),$$
$$R_5=\int_0^\infty dr\ r^2 g_{W',\kappa'}(r)f_{-W,\kappa}(r)h^{(1)}_L(\omega r),$$
$$R_6=\int_0^\infty dr\ r^2 f_{W',\kappa'}(r)g_{-W,\kappa}(r)h^{(1)}_L(\omega r). \tag{26}$$

In the case of a pointlike nucleus, these integrals can be rewritten in terms of F_2 functions [4] which can be evaluated numerically. For the representation of the nucleus as a homogeneously charged sphere, the radial integrals are computed using a Gauss-Chebyshev quadrature [16]. The Whittaker functions which occur in the expressions for the electron wave functions are computed with the COULCC code of [17]. Since the integrands are oscillating functions, it is advantageous to deform the integration contour in the complex plane in such a way that it runs along the imaginary axis [5]. Since the electron wave functions have the asymptotic behavior $\exp(ipr)$ while the Hankel functions behave like $\exp(i\omega r)$, where $\omega=W+W'$, the integrand for large r assumes the form

$$\exp(i[-p-p'+W+W']r). \tag{27}$$

For r complex with the imaginary part going to infinity, our procedure thus guarantees that the integrand falls off quite fast. In most cases at $r=20\,000$ fm, the integrand is smaller than 10^{-5} of its maximum value.

We want to consider the angular correlation for two special cases.

(I) If we integrate Eq. (23) over the positron polar angle ϑ and the dihedral angle δ, the remaining function depends only on the opening angle Θ of the electron-positron pair. In this case only the $n=0$ contribution survives. We get the opening angle distribution as a series of Legendre polynomials which was already calculated in [18]:

$$\frac{d^2\beta}{dE\ d\cos\Theta}=\sum_I a_I P_I(\cos\Theta). \tag{28}$$

The expansion coefficients are given by

$$a_I=\frac{8\pi\alpha\omega}{L(L+1)}(-)^{L+I+1}(2I+1)\sum_{\kappa,\kappa',\overline{\kappa},\overline{\kappa'}}|\kappa\kappa'\overline{\kappa}\overline{\kappa'}|$$
$$\times R^{(\tau)}_{\kappa'\kappa}(L)R^{(\tau)*}_{\overline{\kappa'}\overline{\kappa}}\exp\{i[\delta'(W',\kappa')-\overline{\delta'}(W',\overline{\kappa'})$$
$$+\delta(-W,\kappa)-\overline{\delta}(-W,\overline{\kappa})]\}\begin{pmatrix}j' & \overline{j'} & I\\ 1/2 & -1/2 & 0\end{pmatrix}$$
$$\times\begin{pmatrix}j & \overline{j} & I\\ 1/2 & -1/2 & 0\end{pmatrix}\begin{pmatrix}j & j' & L\\ 1/2 & -1/2 & 0\end{pmatrix}$$
$$\times\begin{pmatrix}\overline{j} & \overline{j'} & L\\ 1/2 & -1/2 & 0\end{pmatrix}\begin{Bmatrix}\overline{j} & \overline{j'} & L\\ j' & j & I\end{Bmatrix}. \tag{29}$$

They have to be evaluated numerically. The same result is achieved if one assumes that the initial nuclear substates are equally populated.

At this point we apologize for giving an incorrect expression for the opening angle distribution in [18], which was caused by employing the wrong set of scattering solutions. This error resulted in the wrong sign of the scattering phase shifts of the positron. The opening angle distribution showed the right qualitative behavior, but wrong conversion probabilities. The statement that the maximum of the distribution shifts from 0° to 180°, if one considers overcritical nuclear charges ($Z \geqslant 173$), remains unchanged. This error appeared also in the expression for the electric monopole ($E0$) conversion. One should reverse the sign of the scattering phase shifts of the positron. The pair conversion coefficient for the electric monopole conversion reads

$$\frac{d\eta}{dE\ d\ \cos\Theta} = \frac{1}{2}\frac{d\eta}{dE}\,(1+\epsilon\ \cos\Theta), \tag{30}$$

where $d\eta/dE$ is the differential pair conversion coefficient [6]—which remains unchanged—and ε is the corrected anisotropy coefficient:

$$\varepsilon = 2\,\frac{C_{-1}C_{+1}}{C_{-1}^2+C_{+1}^2}\,\cos(\Delta_{+1-1}), \tag{31}$$

with

$$\Delta_{\kappa\kappa'} = \delta'(W',\kappa) - \delta'(W',\kappa') + \delta(-W,\kappa) - \delta(-W,\kappa'). \tag{32}$$

C_{+1}, C_{-1} are defined by

$$C_\kappa = \begin{cases} \lim\limits_{r\to 0} \dfrac{f_{-W,\kappa}(r) f'_{W',\kappa}(r)}{r^{2j-1}} & \text{for } \kappa > 0, \\ \lim\limits_{r\to 0} \dfrac{g_{-W,\kappa}(r) g'_{W',\kappa}(r)}{r^{2j-1}} & \text{for } \kappa < 0, \end{cases} \tag{33}$$

where f (f') and g (g') are the radial wave functions of the Dirac spinor of the positron (electron). In numerical calculations these constants are evaluated at the nuclear radius. δ and δ' are the corresponding Coulomb phase shifts for an extended nucleus [19].

(II) If we integrate Eq. (23) over the opening angle Θ of the electron-positron pair and the dihedral angle δ, we end up with

$$\frac{d^2\beta}{dE\ d\ \cos\vartheta} = \sum_n\ b_n P_n(\cos\vartheta), \tag{34}$$

where the coefficients read

$$\begin{aligned} b_n = {} & 4\pi\alpha\omega\ \frac{(2L+1)(2J_i+1)}{L(L+1)}\,(-)^{J_f-J_i+1}\sqrt{2n+1}\,\hat{\rho}_0^{[n]}(J_i) \\ & \times \begin{Bmatrix} L & L & n \\ J_i & J_i & J_f \end{Bmatrix} \sum_{\kappa,\kappa',\overline{\kappa}} (-)^{j+\overline{j}+j'+1/2} \left| \kappa\kappa'\overline{\kappa} \right| \\ & \times \begin{Bmatrix} L & L & n \\ j & \overline{j} & j' \end{Bmatrix} R^{(\tau)}_{\kappa'\kappa}(L) R^{\tau *}_{\kappa'\overline{\kappa}}(L) \\ & \times \exp\{i[\,\delta(-W,\kappa) - \overline{\delta(-W,\kappa)}]\} \begin{pmatrix} j & \overline{j} & n \\ 1/2 & -1/2 & 0 \end{pmatrix} \\ & \times \begin{pmatrix} j & j' & L \\ 1/2 & -1/2 & 0 \end{pmatrix} \begin{pmatrix} \overline{j} & j' & L \\ 1/2 & -1/2 & 0 \end{pmatrix}. \end{aligned} \tag{35}$$

This corresponds to the experimental setup where one is just interested in the angular distribution of the positron emitted in internal pair conversion of an aligned or polarized nucleus.

V. RESULTS

In the following we will discuss the characteristic properties of IPC angular distributions using a few representative results. Since we are interested in Coulomb effects, they all refer to a uraniumlike nucleus ($Z=92$). The chosen energies and multipolarities are generic and are not intended to represent particular nuclear transitions known from experiment.

The opening angle distribution of electron and positron emitted by IPC depicts for electric transitions the typical pattern: It has its maximum at $\Theta = 0°$ and its minimum for $\Theta = 180°$. For magnetic transitions in heavy nuclei, however, the situation might be different. Figures 1(a) and 1(b) depict the opening angle distribution for an $E1$ and an $M1$ transition of a uraniumlike nucleus as a result of our distorted wave Born approximation (DWBA) in comparison with the Born approximation (BA). This demonstrates how the angular correlation of the electron-positron pairs is influenced by the strong Coulomb field of the nucleus. In Fig. 1(b) we plotted also the opening angle distribution for the $M1$ transition taking into account the finite extension of the nucleus under consideration. This verifies that the magnetic transitions—and especially the $M1$ transition—are very sensitive to the charge distribution of the nucleus [5]. For the $E1$ transition in Fig. 1(a), on the other hand, the effect of the finite nuclear size amounts to less than 0.1%.

In the following we discuss the triple angular correlation of electron and positron for IPC of aligned nuclei. We take the symmetry axis as quantization axis as in Eq. (23). The opening angle Θ of electron and positron, the polar angle ϑ of the positron, and the dihedral angle δ form a complete set of angles to fix the emission directions of electron and positron with respect to the symmetry axis. The angles which describe the directions of the emitted leptons are displayed in Fig. 2(b). Note that our choice of the coordinate system is different from that introduced in the Born approximation calculations of [1–3] in which ϑ denotes the polar angle of the intermediate photon. However, since the Coulomb field disturbs the momentum balance, we cannot determine the momentum of the intermediate photon from the momenta of the

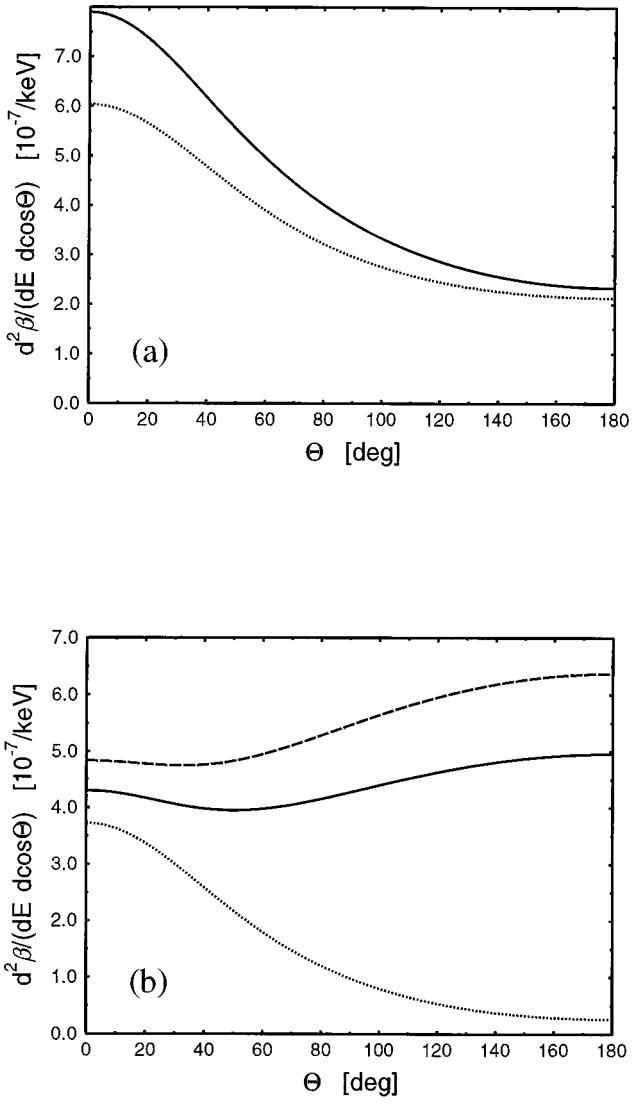

FIG. 1. Opening angle distribution of electron-positron pairs emitted by IPC of randomly oriented uraniumlike nuclei (a) for an $E1$ transition, (b) for an $M1$ transition. The transition energy amounts in both cases to 2 MeV, and the kinetic positron energy was taken to be 800 keV. The solid lines correspond to the DWBA calculations, and dotted lines display the outcome of the Born approximation. The effect of the finite nuclear extension in the case of $M1$ transitions can be deduced from the dashed line which reflects the point nucleus approximation.

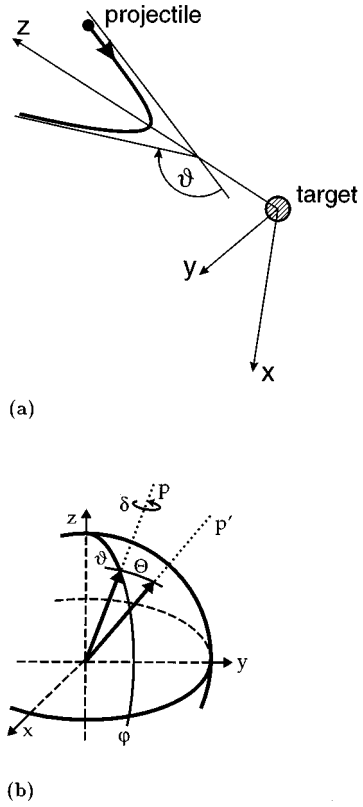

FIG. 2. (a) The coordinate system which is chosen to describe the alignment of the Coulomb excited nuclei in heavy-ion collisions. ϑ denotes here the scattering angle of the projectile in the laboratory system. (b) Definition of the angles which are used to describe the directions of electron and positron in space. Θ is the opening angle of the electron-positron pair, ϑ denotes the polar angle of the positron with respect to the quantization axis, and the dihedral angle δ indicates the angle about which the electron-positron emission plane is rotated around the positron axis.

outgoing leptons, which would be necessary to calculate the photon polar angle.

Depending on the experimental setup and reactions, various coordinate systems may be established in which the statistical tensors are determined. Here we concentrate on the Coulomb excitation of heavy ions in collisions with beam energies at or below the Coulomb barrier. In this case one usually chooses a coordinate system, where the z axis is pointing along the apex line of the scattering hyperbola towards the projectile and the x axis is perpendicular to the scattering plane [Fig. 2(a)]. The y axis is then chosen such that the y component of the projectile velocity is positive [7,8,20]. In the sudden approximation it can be shown that the nuclear states are excited with a population of the magnetic substates reaching a maximum around $M_i=0$; i.e., the nucleus is aligned in the plane perpendicular to the z axis (asymptotic recoil direction of the target) [15]. This is called oblate alignment. Taking into account the deexcitation of the nucleus by γ cascades starting from high spin, the oblate alignment changes into a prolate alignment with respect to the z axis for the low-spin states.

If the collision energy is increased, the nuclear alignment changes to a polarization with respect to a reference axis perpendicular to the scattering plane [8,20]. Classically, this corresponds to the situation where the drag caused by surface friction puts the nuclei into a spinning motion.

After having chosen a coordinate system and having determined the degree of alignment or polarization for the Coulomb excited nuclei—the corresponding statistical tensors can be calculated with, e.g., the COULEX code of [7]—one can employ Eq. (23) to determine the angular distribution of the electron-positron pairs emitted by internal pair conversion of these nuclei. We plot in Fig. 3 the spatial correlation of the electron-positron pairs with respect to the reference axis assuming oblate alignment of a uraniumlike nucleus. From the spectrum of the emitted pairs [5,21], we know that for large-Z nuclei the pair emission probability increases to-

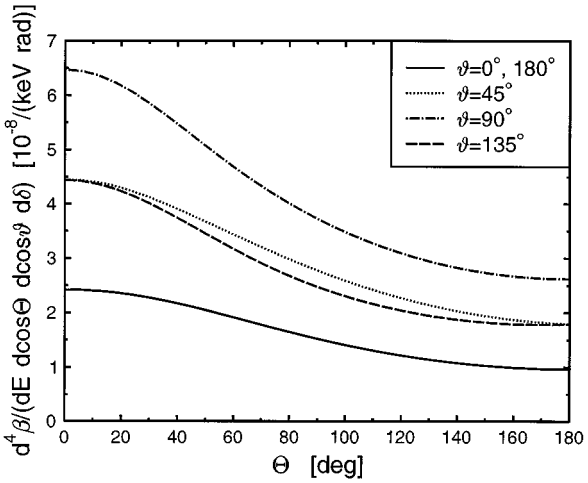

FIG. 3. Angular correlation of electron-positron pairs in $E1$-IPC for a transition from a 1^- to a 0^+ state, assuming oblate alignment of uraniumlike nuclei in the initial state. The conversion probability is plotted versus the opening angle of the emitted lepton pair for various polar angles of the positron with respect to the z axis. The transition energy amounts to $\omega=1800$ keV, the kinetic positron energy to $E=700$ keV. The dihedral angle δ was fixed to 0°.

wards the maximum positron energy. Thus the angular correlations are plotted for a case where nearly the full transition energy (minus the electron rest mass) is transferred to the positron. One recognizes a strong dependence of the pair conversion probability on the polar angle of the positron with respect to the reference axis. This behavior resembles the anisotropic emission of the intermediary photon [15]. The angular distribution depends weakly on the dihedral angle δ of the electron-positron pair (Fig. 4). For transitions between nuclear states of high angular momentum, the opening angle distribution does not change drastically when the positron polar angle is varied.

In order to elucidate the influence of the statistical tensors,

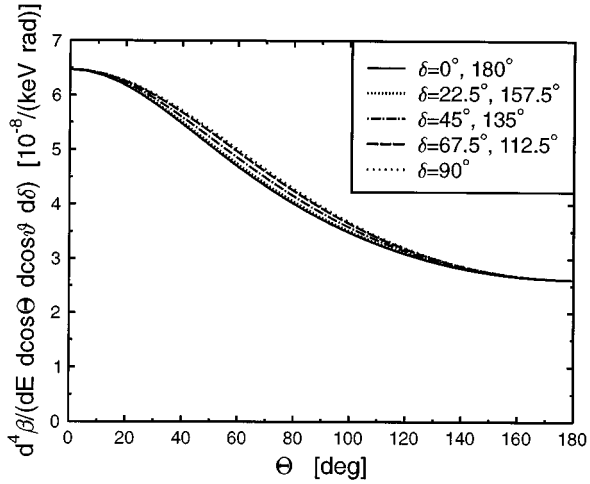

FIG. 4. Angular correlation of electron-positron pairs in $E1$-IPC for the same transition and energies as in Fig. 3. The pair conversion probability is plotted for fixed polar angle $\vartheta=90°$ and several values of the dihedral angle δ.

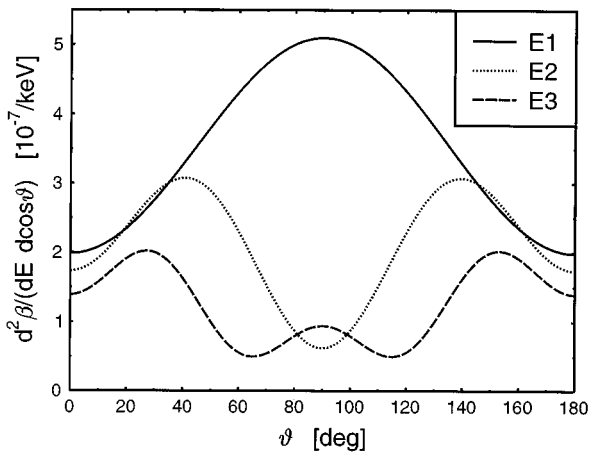

FIG. 5. Polar angle distribution assuming $E1$, $E2$, and $E3$ transitions to the 0^+ ground state of a nucleus showing oblate alignment. The transition energy amounts to 1800 keV, the kinetic positron energy was fixed to 700 keV.

i.e., the occupation of the initial nuclear state on the angular correlation of the emitted electron-positron pairs, we present the angular distribution with respect to the polar angle of the emitted positron. Figure 5 shows the polar angle distribution assuming $E1$, $E2$, and $E3$ transitions to the 0^+ ground state of nuclei which exhibit oblate alignment. Figure 6 displays the polar angle distribution for a $E1$ transition to the 0^+ ground state of a nucleus for oblate and prolate alignment and for polarization.

VI. CONCLUSION

We presented the first calculation of the spatial correlation of electron-positron pairs emitted in internal pair conversion in heavy nuclei, which consistently takes into account the strong Coulomb field of finite size nuclei. The angular correlation of electron-positron pairs with respect to a given axis in space was derived in terms of statistical tensors which

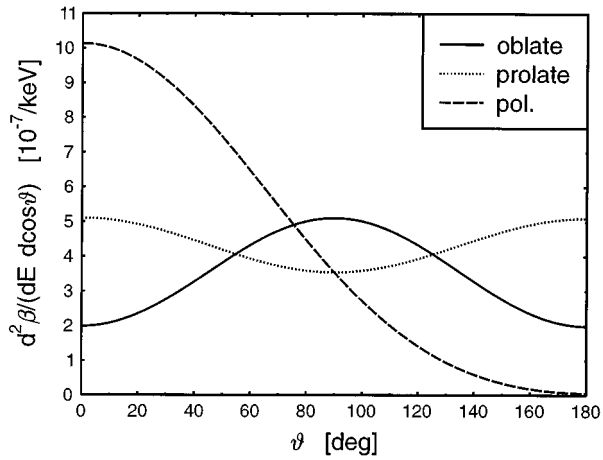

FIG. 6. Polar angle distribution assuming an $E1$ transition to the 0^+ ground state of a nucleus with oblate alignment, prolate alignment, and polarization. The transition energy amounts to 1800 keV, the kinetic positron energy to 700 keV.

reflect the population of the nuclear magnetic substates. The conversion probability changes drastically when either the opening angle of the pair or the polar angle of the positron is varied while the dependence on the dihedral angle is rather weak.

With our computations the results of Goldring [1], Rose [2], and Warburton [3], which were obtained within Born approximation, i.e., $Z=0$, could be extended up to nuclear charge numbers far beyond the critical value of $Z=173$ [19]. For nuclear charge numbers in the regime of lead and uranium, we obtained striking deviations to the angular correlation derived within Born approximation which was already expected from the electron-positron pair spectra calculated earlier [4,5]. The Born approximation cannot be considered as being valid in this regime. In particular, this is verified by the opening angular distribution of the electron-positron pairs resulting from nuclear $M1$ transitions which exhibits a maximum yield for back-to-back emission, whereas the Born approximation predicts a minimum. Furthermore, in the case of magnetic transitions we find a strong dependence of the pair emission rate on the nuclear size.

Our calculations concerning the spatial correlation supplement the well-known results from γ-ray angular correlation experiments in heavy-ion collisions. We emphasize that the shape of the electron-positron angular correlation can be employed to deduce the population probabilities of the nuclear rotational substates and thus to discriminate prolate and oblate alignment as well as to determine the multipolarity of nuclear transitions. This complements the outcome from γ-ray spectroscopy. The angular correlation of positrons integrated over the spatial electron angle resembles the typical photon distribution. The difference in shape is caused by longitudinally polarized photons which occur as intermediate state in internal pair conversion. The so-called longitudinal matrix elements are a new feature which yields additional informations. Since the γ-ray angular distribution involves just even-rank statistical tensors, it does not allow one to discriminate between alignment and polarization. One may overcome this shortcoming by measuring either the photon polarizations or, as suggested by our calculations, by studying the electron-positron pair distribution.

Applied to the electron-positron coincidence experiments currently analyzed at GSI (Darmstadt) and at Argonne, our presented results can be utilized to determine precisely the nuclear background contribution. Since all the experimental setups are now equipped with detectors for the angular distribution of emitted particles, the experimental collaborations rely on accurate theoretical results of the various processes that contribute to the recorded spectra.

ACKNOWLEDGMENTS

This work has been supported by the BMBF, by the Deutsche Forschungsgemeinschaft (DFG), by GSI (Darmstadt), and by the REHE program of the European Science Foundation (ESF).

APPENDIX A: ELECTRON WAVE FUNCTIONS FOR POINTLIKE AND EXTENDED NUCLEI

In our calculations we employed the following form of the spherical continuum wave functions of the electron moving in the Coulomb field of a pointlike nucleus [22]:

$$\chi_{W,\kappa,\mu}(\vec{r})=\begin{pmatrix} g_{W,\kappa}(r)\chi_{\kappa\mu}(\hat{r}) \\ if_{W,\kappa}(r)\chi_{-\kappa\mu}(\hat{r}) \end{pmatrix}. \tag{A1}$$

The spinor spherical harmonics are defined as

$$\chi_{\kappa\mu}(\Omega)=\sum_{\kappa,\mu}\begin{pmatrix} l & 1/2 & \left| j \right. \\ m & \lambda & \left| \mu \right. \end{pmatrix} Y_{\lambda m}(\Omega)\chi_{\lambda}, \tag{A2}$$

where the basis spinors are given as usual by

$$\chi_{1/2}=\begin{pmatrix}1\\0\end{pmatrix}, \quad \chi_{-1/2}=\begin{pmatrix}0\\1\end{pmatrix}. \tag{A3}$$

Defining the relativistic Sommerfeld parameter as $y=-Z\alpha W/p$ where $p=\sqrt{W^2-m^2}$, the radial wave functions read, for a point nucleus,

$$\begin{aligned} g_{W,\kappa}(r)=&\sqrt{\frac{W+m}{\pi p}}\frac{1}{r}\frac{|\Gamma(\gamma-iy)|}{2\Gamma(2\gamma+1)} \\ &\times e^{-\pi y/2}(2pr)^{\gamma}\{(\gamma-iy)e^{-i(pr-\eta)} \\ &\times {}_1F_1(\gamma+1-iy,2\gamma+1;2ipr)+\text{c.c.}\}, \\ f_{W,\kappa}(r)=&\sqrt{\frac{W-m}{\pi p}}\frac{i}{r}\frac{|\Gamma(\gamma-iy)|}{2\Gamma(2\gamma+1)} \\ &\times e^{-\pi y/2}(2pr)^{\gamma}\{(\gamma-iy)e^{-i(pr-\eta)} \\ &\times {}_1F_1(\gamma+1-iy,2\gamma+1;2ipr)-\text{c.c.}\}, \end{aligned} \tag{A4}$$

with

$$\eta=\frac{1}{2}\arg\left(-\frac{\kappa+iym/W}{\gamma-iy}\right), \quad \gamma=\sqrt{\kappa^2-(Z\alpha)^2}.$$

For an extended nucleus we construct the continuum solutions as in [19] by employing a power series ansatz for the electron wave function inside the nucleus which is matched to the linear combination of wave functions to the Coulomb potential at the nuclear radius. From the matching condition the normalization factor and the phase shift can be deduced.

The continuum solutions of the Dirac equation can be written as wave functions which asymptotically represent plane waves of momentum $\vec{p}$ and spin λ. These wave functions are obtained as a series expansion into spherical harmonics [22,23].

For positive energies this expansion reads

$$\psi^{(\pm)}_{W,\vec{p},\lambda}=\sum_{\kappa,\mu} a^{(\pm)}_{\kappa\mu}\chi_{W,\kappa,\mu}, \tag{A5}$$

with the coefficients

$$a^{(\pm)}_{\kappa\mu}=\frac{1}{\sqrt{Wp}}\, i^l e^{\pm i[\delta(W,\kappa)+\pi(l+1)/2]}\sum_m Y^*_{lm}(\hat{p})\begin{pmatrix} l & 1/2 & \left| j \right. \\ m & \lambda & \left| \mu \right. \end{pmatrix} \tag{A6}$$

and the Coulomb phase shift

$$\delta(W,\kappa)=\eta-\arg\Gamma(\gamma-iy)-\frac{\pi}{2}\,\gamma \tag{A7}$$

and, for negative energies ($-W<0$) [23],

$$\psi^{(\pm)}_{-W,\vec{p},\lambda}=\sum_{\kappa,\mu} b^{(\pm)}_{\kappa\mu}\chi_{-W,\kappa,\mu}\,, \tag{A8}$$

with the coefficients

$$b^{(\pm)}_{\kappa,\mu}=\frac{1}{\sqrt{Wp}}\,i^{l(-\kappa)+1}e^{\pm i[\delta(-W,\kappa)+\pi l(-\kappa)]}\sum_m\; Y^*_{l(-\kappa)m}(\hat{p}) \times\begin{pmatrix} l(-\kappa) & 1/2 & \left| j \right. \\ m & \lambda & \left| \mu \right. \end{pmatrix} \tag{A9}$$

and the Coulomb phase shift

$$\delta(-W,\kappa)=\eta-\arg\Gamma(\gamma-iy)-\frac{\pi}{2}\,\gamma. \tag{A10}$$

These wave functions obey the normalization condition

$$\int\; d^3r[\,\psi^{(\pm)}_{W,\vec{p},\lambda}(\vec{r})]^\dagger\psi^{(\pm)}_{W',\vec{p}',\lambda'}(\vec{r})=\delta^3(\vec{p}-\vec{p}\,')\,\delta_{\lambda\lambda'}\,. \tag{A11}$$

In the case of an extended nucleus, the phase shifts have to be determined numerically.

APPENDIX B: EVALUATION OF THE COEFFICIENTS *A* AND *B*

We start with the coefficients A, which contain the electron scattering wave function and its complex conjugate. Inserting the explicit form of these coefficients, Eq. (A6), we get

$$\begin{aligned} A_{\kappa'\mu';\overline{\kappa'}\,\overline{\mu'}}=&\sum_{\lambda',m',\overline{m'}}\;\exp\{i[\,\delta'(W',\kappa')-\overline{\delta'}(W',\overline{\kappa'})]\} \\ &\times\sqrt{2j'+1}\,\sqrt{2\overline{j'}+1}\,(-1)^{l'(\kappa')-1/2+\mu'} \\ &\times Y_{l'(\kappa')m'}(\Omega_{p'})Y^*_{\overline{l'}(\overline{\kappa'})\overline{m'}}(\Omega_{p'}) \\ &\times(-1)^{\overline{l'}(\overline{\kappa'})-1/2+\overline{\mu'}}\begin{pmatrix} l'(\kappa') & 1/2 & j' \\ m' & \lambda' & -\mu' \end{pmatrix} \\ &\times\begin{pmatrix} \overline{l'}(\overline{\kappa'}) & 1/2 & \overline{j'} \\ \overline{m'} & \lambda' & -\overline{\mu'} \end{pmatrix}, \end{aligned} \tag{B1}$$

which can be transformed into

$$\begin{aligned} A_{\kappa'\mu';\overline{\kappa'}\,\overline{\mu'}}=&\frac{1}{\sqrt{4\pi}}\,\exp\{i[\,\delta'(W',\kappa')-\overline{\delta'}(W',\overline{\kappa'})]\} \\ &\times(-1)^{\mu'+1/2}\sqrt{2j'+1}\,\sqrt{2\overline{j'}+1} \\ &\times\sum_{I',\alpha'}\;\sqrt{2I'+1}\,Y_{I'\alpha'}(\Omega_{p'})\begin{pmatrix} j' & \overline{j'} & I' \\ 1/2 & -1/2 & 0 \end{pmatrix} \\ &\times\begin{pmatrix} \overline{j'} & j' & I' \\ -\overline{\mu'} & \mu' & -\alpha' \end{pmatrix}. \end{aligned} \tag{B2}$$

Additionally, we get the parity selection rule

$$l'(\kappa')+\overline{l'}(\overline{\kappa'})+I'=0\;\;\mathrm{mod}\;\;2$$

and the angular momentum selection rule

$$|l'(\kappa')-\overline{l'}(\overline{\kappa'})|\leq I'\leq l'(\kappa')+\overline{l'}(\overline{\kappa'}).$$

Next, we proceed to evaluate the coefficients B, which are composed from the positron scattering wave functions, Eq. (A9):

$$\begin{aligned} B_{\kappa\mu;\overline{\kappa\mu}}=&\sum_{m,\overline{m}\lambda}\;(-1)^{1+\mu+\overline{\mu}}\exp\{i[\,\delta(-W,\kappa) \\ &-\delta(-W,\overline{\kappa})]\}\sqrt{2j+1}\,\sqrt{2\overline{j}+1}\,Y^*_{l(-\kappa)m}(-\Omega_p) \\ &\times Y_{\overline{l}(-\overline{\kappa})\overline{m}}(-\Omega_p)\begin{pmatrix} l(-\kappa) & 1/2 & j \\ m & -\lambda & -\mu \end{pmatrix} \\ &\times\begin{pmatrix} \overline{l}(-\overline{\kappa}) & 1/2 & \overline{j} \\ \overline{m} & -\lambda & -\overline{\mu} \end{pmatrix}. \end{aligned} \tag{B3}$$

This can be rewritten as

$$\begin{aligned} B_{\kappa\mu;\overline{\kappa\mu}}=&(-1)^{\overline{\mu}+1/2}\,\frac{1}{\sqrt{4\pi}}\,\exp\{i[\,\delta(-W,\kappa) \\ &-\overline{\delta}(-W,\overline{\kappa})]\}\sqrt{2j+1}\,\sqrt{2\overline{j}+1}\sum_{I,\alpha}\;\sqrt{2I+1}\,Y_{I\alpha}(\Omega_p) \\ &\times\begin{pmatrix} j & \overline{j} & I \\ 1/2 & -1/2 & 0 \end{pmatrix}\begin{pmatrix} \overline{j} & j & I \\ -\overline{\mu} & \mu & \alpha \end{pmatrix}. \end{aligned} \tag{B4}$$

Furthermore, we obtain the parity and angular momentum selection rules

$$l(-\kappa)+\overline{l}(-\overline{\kappa})+I=0\;\;\mathrm{mod}\;\;2,$$

$$|l(-\kappa)-\overline{l}(-\overline{\kappa})|\leq I\leq l(-\kappa)+\overline{l}(-\overline{\kappa}).$$

[1] G. Goldring, Proc. Phys. Soc. London A **66**, 341 (1953).
[2] M. E. Rose, Phys. Rev. **131**, 1260 (1963).
[3] E. K. Warburton, Phys. Rev. **133**, B1368 (1964).
[4] P. Schlüter, G. Soff, and W. Greiner, Z. Phys. A **286**, 149 (1978).
[5] P. Schlüter, G. Soff, and W. Greiner, Phys. Rep. **75**, 327 (1981).
[6] G. Soff, P. Schlüter, and W. Greiner, Z. Phys. A **303**, 189 (1981).
[7] *Coulomb Excitation*, edited by K. Alder and A. Winther (Academic, New York, 1966).
[8] K. Alder and A. Winther, *Electromagnetic Excitation* (North-Holland, Amsterdam, 1975).
[9] R. Bär, A. Balanda, J. Baumann, W. Berg, K. Bethge, H.

Bokemeyer, H. Folger, O. Fröhlich, R. Ganz, O. Hartung, M. Samek, P. Salabura, W. Schön, D. Schwalm, K. Stiebing, P. Thee, E. Berdermann, F. Heine, S. Heinz, O. Joeres, P. Kienle, I. Koenig, W. Koenig, C. Kozhuharov, U. Leinberger, A. Schröter, and H. Tsertos, Nucl. Phys **A583**, 237 (1995).

[10] I. Ahmad, S. M. Austin, B. B. Back, R. R. Betts, F. P. Calaprice, K. C. Chan, A. Chishti, P. Chowdhury, C. Conner, R. W. Dunford, J. D. Fox, S. J. Freedman, M. Freer, S. B. Gazes, A. L. Hallin, T. Happ, D. Henderson, N. I. Kaloskamis, E. Kashy, W. Kutschera, J. Last, C. J. Lister, M. Liu, M. R. Maier, D. J. Mercer, D. Mikolas, P. A. A. Perera, M. D. Rhein, D. E. Roa, J. P. Schiffer, T. A. Trainor, P. Wilt, J. S. Winfield, M. Wolanski, F. L. H. Wolfs, A. H. Wuosmaa, G. Xu, A. Young, and J. E. Yurkon, Phys. Rev. Lett. **75**, 2658 (1995).

[11] M. E. Rose, *Angular Momentum Theory* (Wiley, New York, 1957).

[12] J. M. Eisenberg and W. Greiner, *Nuclear Theory 1: Nuclear Models* (North-Holland, Amsterdam, 1987).

[13] L. C. Biedenharn, in *Nuclear Spectroscopy B*, edited by F. Ajzenberg-Selove (Academic, New York, 1960).

[14] D. Pelte and D. Schwalm, in *Heavy Ion Collisions*, edited by R. Bock (North-Holland, Amsterdam, 1991), Vol. 3, p. 1.

[15] H.-J. Wollersheim, GSI Report No. GSI-93-22, 1993.

[16] J. M. Perez-Jorda, E. San-Fabian, and F. Moscardo, Comput. Phys. Commun. **70**, 271 (1992).

[17] A. R. Barnett and I. J. Thompson, Comput. Phys. Commun. **36**, 363 (1985).

[18] C. Hofmann, J. Reinhardt, W. Greiner, P. Schlüter, and G. Soff, Phys. Rev. C **42**, 2632 (1990).

[19] B. Müller, J. Rafelski, and W. Greiner, Nuovo Cimento A **18**, 551 (1973).

[20] R. A. Broglia and A. Winther, *Heavy Ion Reactions* (Addison-Wesley, Redwood City, CA, 1991).

[21] P. Schlüter and G. Soff, At. Data Nucl. Data Tables **24**, 509 (1979).

[22] M. E. Rose, *Relativistic Electron Theory* (Wiley, New York, 1961).

[23] C. Hofmann, J. Augustin, J. Reinhardt, A. Schäfer, W. Greiner, and G. Soff, Phys. Scr. **48**, 257 (1993).